ACS APPLIED MATERIALS & INTERFACES

Research Article

www.acsami.org

Use of Free Radicals on the Surface of Plasma Polymer for the Initiation of a Polymerization Reaction

Farid Khelifa, Sergey Ershov, Youssef Habibi,* Rony Snyders, and Philippe Dubois*

Institute of Research in Science and Engineering of Materials, University of Mons - UMONS, Place du Parc, 23, 7000 Mons, Belgium

ABSTRACT: A novel approach to functionalize plasma polymer films (PPFs) through the grafting polymerization initiated from free radicals trapped in the film was developed in this work. 2-Ethylhexyl acrylate (EHA) was chosen as radically polymerizable monomer given the wide use of its corresponding polymer in coating and adhesive applications. The occurrence of the grafting was first confirmed by time-of-flight secondary ion mass spectrometry (ToF-SIMS) and X-ray photoelectron spectroscopy (XPS). Then grafted chains were studied in more detail. The thickness of grafted chains was quantitatively estimated by angle-resolved XPS (ARXPS), while their morphology and interfacial behavior were qualitatively investigated by atomic force microscopy (AFM), contact angle measurements, and quartz crystal microbalance (QCM). The latter technique provided additional insights regarding the swelling behavior of the grafted layer and its stability upon exposure to challenging environments. Reported scientific findings suggest to use this approach for the covalent binding of a very thin layer on the top surface of a PPF without affecting its bulk properties.

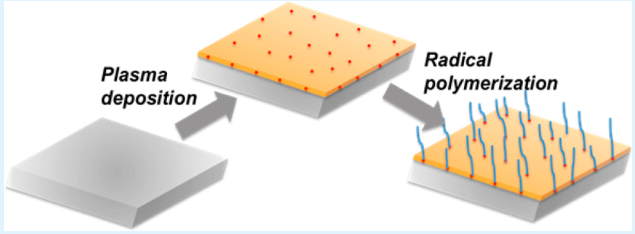

KEYWORDS: *plasma polymer film, free radical, polymerization, grafting, acrylics*

INTRODUCTION

During many years, extensive research was performed on plasma polymer films (PPFs) providing valuable details on the formation of unsaturation and the occurrence of insolubility due to a cross-linked structure.[1−3] Nowadays, PPFs are widely used in various fields for coating of solidlike membranes, semiconductors, metals, textiles, or polymers due to their excellent adhesion properties. The versatility of plasma polymerization lies in the possibility to produce films with the thickness ranging from several nanometers to micrometers, while specific properties such as antifogging, adhesion, anticorrosion, chemical, or scratch resistance can be achieved merely by the proper selection of the precursor building blocks. For example, thin polymer-like coatings were recently produced by plasma enhanced chemical vapor deposition (PECVD) as barrier or corrosion-inhibiting coatings for aluminum in automotive industry.[4−6] The major difference of the plasma polymer from conventional polymers is the absence of a repeating (molecular) unit in their structure. Indeed, plasma polymers are characterized by a highly cross-linked structure responsible for an enhanced chemical stability as well as good mechanical resistance. Nevertheless, due to the chemical bond dissociation characteristics of the growth mechanism[7−9] that generates free radicals (trapped) within the PPF, the main concern with the PPF is the aging phenomenon induced by the postoxidation occurring during the course of use. Initially, oxygen present in the PPF synthesized from oxygen-free precursors was thought to arise from the residual oxygen or the water vapor present in the plasma reactor. However, it has been shown that the oxygen uptake originates primarily from the reaction between the trapped free radicals and oxygen upon exposure of the PPF to the air.[10−14]

It is well-known that plasma-based treatments are widely used for incorporation of reactive functional groups on the surfaces of polymer-based materials in order to enhance adhesive properties of polymers like polyethylene.[15−17] These plasma treatments have been carried out mainly with nonpolymerizable gases such as O_2, N_2, or NH_3 that lead to generation of corresponding chemical groups; or Ar that induces formation of free radical preactivated polymer surfaces. These free radicals have been exploited to initiate grafting polymerization reaction.[18,19] However, for the PPF deposited by PECVD only a few studies have been reported on the use of free radicals generated during film growth for the initiation of subsequent grafting reaction. To the best of our knowledge, only Teare et al. have successfully initiated radical polymerization from the free radicals present onto the surface of anhydride maleic-based PPF. The authors have shown that the possibility to take advantage of the free radical reactivity is closely linked to the extended lifetime of the radicals induced by resonance phenomena in the anhydride maleic molecule. Free radicals have been subsequently exposed to vapors of amine-based molecules (propylamine or allylamine), and finally, imidization has been performed prior to free radical polymerization. It should be noted that this multistep process is limited only to specific precursors.[20]

Received: June 18, 2013
Accepted: October 22, 2013
Published: October 22, 2013

The present study is part of a bigger research work that aims at developing an organic multilayer coating for corrosion protection purposes. In order to improve the intrinsic properties of aluminum and to increase its resistance to localized corrosion, various coatings have already been developed and successfully implemented on industrial scale. Among those, coatings based on hexavalent chromate have widely been used due to their enhanced corrosion resistance.[21,22] However, hexavalent chromate species have recently been recognized as harmful agents both for the environment and for human beings (carcinogenic). According to Appendix II of the European Directive 2000/53/CE, coatings containing hexavalent chromium shall no longer be used from July 2007.[2] Therefore, coatings displaying similar performances have to be developed and applied for metal protection. An alternative solution could be based on the deposition of a multilayer system with each layer presenting a specific property.

Among these layers, plasma polymers are of particular interest for many reasons, including their good barrier properties and improved adhesion to various substrates including metals. The second layer considered in the global study is a copolymer formed by the 2-ethylhexyl acrylate (EHA) and the glycidyl methacrylate that presents good anticorrosion properties.[23,24] Thus, a covalently grafted layer of poly(EHA) on PPF would serve as an intermediate layer between the plasma film and the subsequent layer of poly(EHA-*co*-GMA). Good compatibilization between the layers is then expected given the same nature of the monomer used in both layers. Hence, in the frame of this work an original and versatile approach to initiate a free radical polymerization of 2-ethylhexyl acrylate in vacuum directly after deposition of an isopropanol-based PPF on a substrate is reported.

In our previous work,[25] the surface free radical density of an isopropanol-based PPF as a function of deposition power was quantitatively evaluated with the help of nitric oxide (NO) chemical derivatization. It was found out that the surface density of free radicals exhibits a maximum for the deposition power of 200 W ($\sim 2.3 \times 10^{14}$ spin/cm^2) followed by its stabilization ($\sim 2.1 \times 10^{14}$ spin/cm^2) with the further power increase.

The novelty of the reported technique lies in the possibility to use a large variety of precursors and monomers. The very few limitations are related to the volatility of the precursor and the ability of the monomer to polymerize via a free radical mechanism. Thus, numerous applications would be possible since a large variety of functionalities can be incorporated on PPF surfaces that can be deposited on wide range of solid substrates. This innovative route to initiate and graft an ultrathin (<5 nm) polymer layer could allow to incorporate specific functionalities as well as to circumvent the reported aging problem[10,12,14] and at the same time to benefit from all the positive aspects of the PPF: adhesion to a large variety of substrates, mechanical resistance, simplicity of tuning the coating properties by varying the precursor(s), resistance to chemicals and solvents, and so forth.

In this work, first the efficiency of polymerization was investigated by time of flight secondary ion mass spectroscopy (ToF-SIMS) and X-ray photoelectron spectroscopy (XPS). Then, optimization of some parameters such as the immersion time in EHA solution was performed. Depth analyses of grafted chains and the study of their interfacial behavior were performed with the help of XPS, quartz crystal microbalance, atomic force microscopy, as well as contact angle measurements.

EXPERIMENTAL SECTION

Materials. PPF was deposited on a p-type (B-doped) Si substrate provided by Siegert wafer GmbH (Germany). 2-Ethylhexyl acrylate (EHA, VWR, 99%) was passed through a basic alumina column to remove the stabilizing agent prior to grafting polymerization experiments. Chloroform (Alfa Aesar, 99+ %), isopropanol (MERCK, 99.8%), and nitric oxide (Air Liquide, 99.9%) were used as received.

PPF Synthesis. After precleaning a silicon wafer with acetone and methanol the PPF was deposited in a lab-scale deposition chamber from an isopropanol gas precursor with a flow rate of 5 sccm (Standard Cubic Centimeters per Minute). The distance between the inductive coil, powered by a CESAR 1310 Generator (Advanced Energy), and the substrate was fixed at 5.5 cm. A base pressure of 10^{-4} Pa was achieved by a combination of scroll and turbomolecular pumps. The working pressure of 6.67 Pa was kept constant during deposition by a throttle valve while the amount of gases (isopropanol, Ar, O_2) in the gas mixture were controlled independently by separate mass flow controllers. Prior to the deposition, substrates were etched for 10 min in an Ar/O_2 discharge (with a flow rate of 25 sccm) at 100 W.

Derivatization Tests. After the deposition, PPF samples were transferred quickly (~3 min) under vacuum into a separate chamber having a base pressure inferior to 10^{-3} Pa for derivatization tests. The labeling agent, nitric oxide (NO), was introduced into the chamber until the pressure of 100 mBar (Pirani gauge controlled) was reached by blocking out of a turbo pump according to the procedure reported previously.[25]

Grafting Experiments. Grafting experiments were performed in the same vacuum chamber as derivatization tests. EHA solution was passed through a basic alumina column to remove the stabilizing agent before being introduced into the chamber through the valve located above the substrate-holder after degassing for 5 min with Ar in order to remove residual oxygen (Figure 1). The pressure was increased with Ar to slightly below atmospheric pressure prior to the introduction of the monomer in order to avoid violent spraying of EHA upon contact with the base vacuum of the chamber and to ensure a complete coverage of the PPF sample by the monomer. The chamber was preheated to 50 °C by an external heater to guarantee efficient polymerization reaction. After polymerization, test samples were washed twice with chloroform for 5 min so that adsorbed layers could be removed before subsequent analyses. Deposition parameters, such as the grafting time and radiofrequency (RF) input power, were investigated.

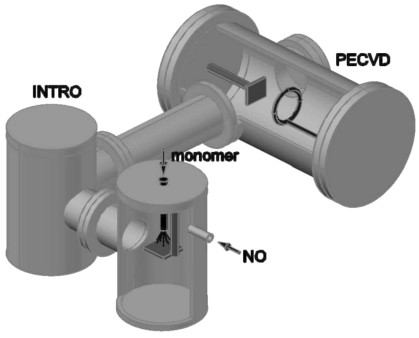

Figure 1. Schematic drawing of the PECVD and derivatization/grafting chambers.

Free Radical Polymerization. In order to obtain a relevant reference for the grafted polymer chains, poly(EHA) was synthesized by a free radical polymerization in THF solution and deposited by spin-coating on a silicon wafer. A detailed description of the polymerization procedure can be found elsewhere.[23]

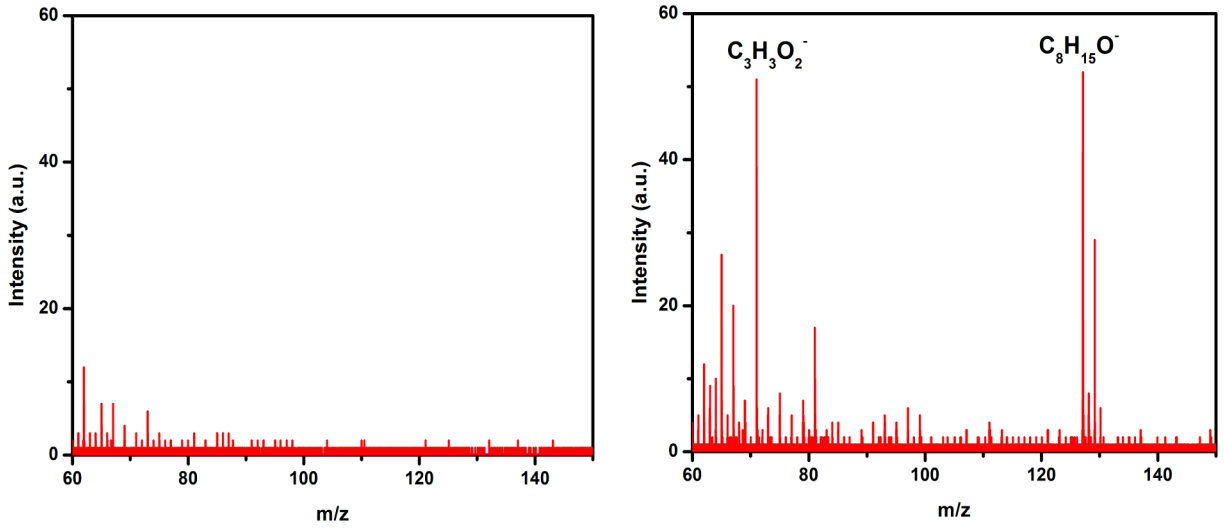

Figure 2. Negative ToF-SIMS spectra of the PPF (left) and the PPF on which poly(EHA) chains were grafted.

Time-of-Flight Secondary Ion Mass Spectrometry (ToF-SIMS). Static ToF-SIMS data of the as-deposited coatings were acquired using a ToF-SIMS IV instrument from ION-TOF GmbH. An Ar^+ 10 keV ion beam at a current of 3.0 pA, rastered over a scan area of 200 × 200 μm^2, was used as analysis beam. The detection was made in the negative ion mode. The resulting spectra exhibit few peaks below m/z = 60 that are not reported here because not really significant neither to the PPF nor to the PPF that underwent a grafting. Therefore, the discussion will be made for the ratio m/z > 60. Five measurements were performed on each sample keeping settings unchanged.

X-ray Photoelectron Spectroscopy (XPS). The chemical composition of the PPF was evaluated by XPS using a Versaprobe PHI 5000 hemispherical analyzer from Physical Electronics with a base pressure below 10^{-7} Pa. The X-ray photoelectron spectra were collected mainly at the takeoff angle of 45° with respect to the electron energy analyzer, operating in constant analyzer energy (CAE) mode (23.5 eV). For angle-resolved experiments, five photoemission angles (relative to the normal to the sample surface) were considered: 0°, 15°, 45°, 60°, and 75°. The spectra were recorded with the monochromatic Al Kα radiation (15 kV, 25 W) with a highly focused beam size of 100 μm. The energy resolution was 0.7 eV, and the binding energy scale of the spectra was calibrated with respect to the aliphatic component of the C1s peak at 285 eV.[26] Eventual surface charging was compensated by a built-in electron gun and an argon ion neutralizer.

Atomic Force Microscopy (AFM). AFM was performed in order to characterize surface topography and to measure physical properties such as adhesion, deformation and dissipation, simultaneously to the height image.[27,28] Films, deposited on silicon wafer, were imaged using peak force tapping (PFT) based on real time force distance curve analysis recorded at a frequency of approximately 2 kHz using a Bruker Nano Inc. ICON atomic force microscope (Santa Barbara, CA) driven by a Nanoscope V control unit, and the tip used was a SNL-10 type in silicon on a nitride lever with a spring constant of 0.35 $N.m^{-1}$ and a radius curvature of about 10 nm. The measurements were realized in air under ambient conditions (temperature and pressure).

Contact Angle Measurements. Contact angle of a water drop on the film's surface was measured using a drop shape analysis system DSA 10 MK2 (Kruss) at room temperature. A drop of deionized water (10 μL) was placed onto the sample surface, and the images of the water menisci on the sample's surface were recorded with a digital camera. These images were analyzed by DSA software in order to obtain contact angle values. A total of 10 measurements in different areas on the surface were averaged.

Quartz Crystal Microbalance. An EG&G Quartz Crystal Analyzer QCA917 apparatus was used as the oscillating circuit and analyzing device in order to measure mass variation (with frequency) of the films upon exposure to different media. The piezoelectric quartz crystal selected for the QCM analysis is a square-shaped crystal model QA-A9M-AU (Ametek). The resonance frequency of the quartz crystal is 9 MHz in AT-cut (polished surface) with gold-plated metal electrodes on both sides and an electrode area of 0.2 cm^2. The oscillator frequency measurement was performed by using a frequency counter with an accuracy of ±1 Hz. For the piezoelectric quartz in use, the Sauerbrey equation[29] was defined (eq 1):

$$\Delta m = (-0.44 \times 10^6) A \frac{\Delta F}{F_0^2} \quad (1)$$

where Δm is the adsorbed mass in g; ΔF is the frequency shift in Hz; F_0 is the fundamental frequency of the quartz, 9 MHz; A is the total sensitive surface of the electrodes, 0.2 cm^2. The constant 0.44 has units of g·MHz·cm^{-2}. The theoretical frequency decrease caused by the adsorption of 1 ng of substance is about 1 Hz.

Prior to deposition and immersion in EHA solution, electrical contacts should be covered in order to avoid their degradation and corrosion. Only one side of the quartz microbalance sensor was coated with the studied material, namely, the PPF with grafted chains of poly(EHA). Thus, PPFs were the deposited on gold QCM sensor and immersed in EHA solution for 1 h at 50 °C as previously detailed. Neat PPF was also deposited. After washing to remove ungrafted chains, the films were dried using nitrogen and introduced in QCM apparatus for measurements. They were then subjected to three cycles of treatments alternating acetone which is a good solvent of poly(EHA) and water which is a poor solvent. Each sample underwent three cycles in each solvent, and each immersion cycle lasted about 20 min. The as-deposited PPF was also subjected to the same set of experiments. At the end, the films were again dried and analyzed to control the mass uptake or loose induced by the immersion in solvents.

RESULTS AND DISCUSSION

Grafting Confirmation. In a previous paper,[25] free radicals present on the surface of the isopropanol-based PPF have been investigated and quantified with the help of NO chemical derivatization in combination with XPS analysis. Derivatization tests revealed that the amount of free radicals increases continuously with P_{RF} up to 200 W (~2.3 × 10^{14} spin/cm^2) before their slight decrease and stabilization at higher powers (to ~2.1 × 10^{14} spin/cm^2 for P_{RF} 300 and 400 W) supposedly due to radical recombination.[14,30] Angle-resolved XPS measurements have shown that primary and secondary radicals are

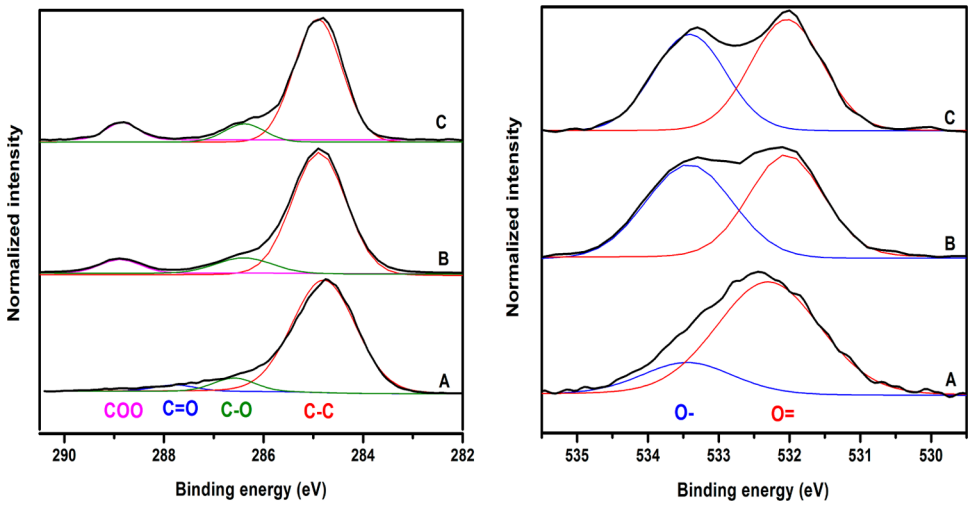

Figure 3. C1s (left) and O1s (right) spectra of the PPF (A), the PPF on which poly(EHA) chains were grafted (B), and a reference of poly(EHA) (C).

dominating on the top surface, while tertiary radicals are present in the subsurface region hidden from the interaction with plasma particles. The increase of the fraction of tertiary radicals with input power has been attributed to the higher fragmentation of the monomer in the discharge, as revealed by in situ plasma phase FTIR spectroscopy, and to the stronger bombardment of the growing film by ions, electrons and VUV photons.

These free radical species generated during PPF synthesis are highly reactive and can undergo oxidation upon exposure to air and, thus, induce aging of the PPF. However, they can also be exploited to initiate radical polymerization, which is namely the focus of the current study, through the free radical polymerization of a vinyl monomer, for example, EHA. Deposition conditions resulting in the maximum of free radicals, previously determined by NO derivatization, were used in order to prove that polymerization is initiated by free radicals trapped in an isopropanol based PPF. So the PPF deposited at 200 W on a silicon wafer was immersed for 1 h in EHA monomer at 50 °C (see Experimental Section) in order to initiate free radical polymerization.

ToF-SIMS has been used in order to characterize the surface of the films. This technique allows investigating qualitatively about 1 nm of the surface of the material. It does not provide quantitative information but can be useful in determining the material present on the extreme surface of the film. Figure 2 presents ToF-SIMS results for the PPF and the PPF as recovered after immersion in EHA for 1 h. At high masses the presence of fragments $C_3H_3O_2^-$ and $C_8H_{15}O^-$ on the PPF surface after immersion in monomer clearly indicates that polymerization of EHA actually took place. Indeed, these fragments $C_3H_3O_2^-$ and $C_8H_{15}O^-$, corresponding to an acrylic group and a long hydrocarbon arm respectively, are characteristic of the EHA molecule. It should be noted that for the nonimmersed PPF these two peaks are absent in the ToF-SIMS spectrum.

More quantitative results from a greater surface depth (~10 nm) than ToF-SIMS can be obtained by XPS analysis. The notable feature of the EHA monomer is the presence in its structure of a carboxylic functional group with a characteristic peak at 289 eV in XPS spectrum. Fortunately, this peak is not present in the C1s spectrum of the PPF. Therefore, the presence of this peak can be considered as an indication that polymerization of EHA was initiated by free radicals generated and trapped during the PPF synthesis. XPS C1s and O1s peaks and the corresponding curve fittings of the bulk poly(EHA) as well as of the as-prepared PPF and the PPF immersed in EHA solution at 50 °C for 1 h are presented in Figure 3. The comparison of C1s spectra shows that the spectrum of the grafted polymer is very similar to the spectrum of the reference poly(EHA), exhibiting likewise the presence of COO peak at 289 eV and C−O peak at 286.5 eV along with the main C−C peak at 285 eV. The C═O peak at 288 eV can be considered as a characteristic peak of the PPF taking into account its considerably reduced contribution to the poly(EHA) spectrum. The comparison of O1s spectra yields similar results − O1s peak shape for the poly(EHA) grafted chains is very close to the reference poly(EHA) (O- and O═ peaks) and is quite different from the PPF (broad peak). This grafting test confirms that free radicals present on the surface of the PPF can efficiently initiate polymerization of radically polymerizable monomers such as acrylates.

Grafting Optimization. In order to optimize the amount of grafted chains that are expected to protect the PPF from oxidation and aging in air, such parameters as RF power for the PPF synthesis and the immersion time in EHA solution have been investigated.

RF power, P_{RF}, is known to have a considerable effect on the degree of the fragmentation of the precursor in plasma. As already mentioned, NO derivatization as well as in situ plasma phase FTIR spectroscopy revealed a continuous increase of P_{RF} up to 200 W implying an increase of precursor fragmentation and, thus, of the amount of free radicals trapped in the film.[25] A further increase of P_{RF} to 300 and 400 W resulted in a decrease of radical amount probably due to the recombination reactions reducing the number of free radicals available for the subsequent derivatization.[14,30]

In order to cross-check the data concerning radical density obtained in NO derivatization experiments, the study of poly(EHA) grafting as function of the P_{RF} was realized. The percentage of COO groups served as an indicator of the polymerization of EHA. Figure 4 shows the alteration of the grafting efficiency represented by COO percentage as a function of P_{RF}. NO derivatization results are also presented

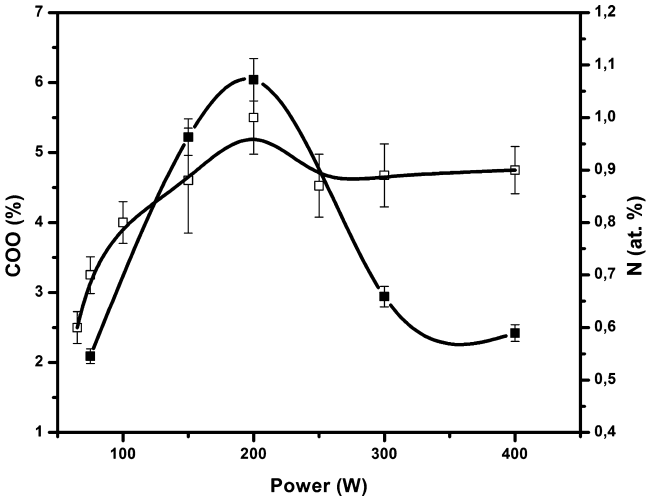

Figure 4. Amount of COO groups as function of the P_{RF} (■) and the amount of nitrogen after NO derivatization (□).

for comparison. The amount of COO increases with power up to 200 W, and then decreases afterward at higher powers. This confirms the results of NO derivatization experiments: isopropanol fragmentation increases with P_{RF} up to 200 W, causing the free radical density to rise before radical recombination takes place at higher powers, reducing the amount of sites available for the initiation of subsequent grafting polymerization. Nevertheless, it should be mentioned that the decrease of COO amount after 200 W for the grafted samples is greater than the decrease of NO amount for the derivatized samples. This difference may be attributed to the fact that either some radicals are quenched by chain termination reactions occurring during polymerization or some radicals trapped within the highly cross-linked PPF subsurface are more accessible for NO molecules that can penetrate deeper into the film than larger EHA molecules.

Grafting experiments for different immersion times in EHA were performed on the PPF deposited at 200 W when the maximum amount of surface free radicals is generated. After the PPF synthesis samples were transferred to the polymerization chamber where they underwent free radical polymerization of EHA during 0 min (PPF), 5 min, 30 min, 60 min, and 24 h. For comparison, a reference sample of poly(EHA) has been synthesized (see Experimental Section) and analyzed by XPS.

After free radical polymerization, PPF samples were thoroughly washed with $CHCl_3$, a good solvent of poly(EHA). This washing procedure allows removing all noncovalently bound polymer chains resulting mainly from radical transfer side-reactions. XPS C1s and O1s peaks of the PPF samples after different immersion times and reference poly(EHA) (not presented here) show that the peak representing the C═O bond, characteristic of the PPF decreases while the peak related to COO of poly(EHA) increases with immersion time. This indicates that the surface of the PPF gets more and more covered by poly(EHA) chains with immersion time. In addition, for the O1s bond two separate contributions characteristics of O− and O═ bonds of the poly(EHA) are observed while for the PPF only one broad peak is present. With the increase of immersion time into EHA the shape of O1s peak of the samples approaches gradually the shape of the poly(EHA) reference.

The integration of the XPS C1s and O1s peaks of the PPF samples after different immersion times in EHA as well as the reference poly(EHA) with the help of a fitting model allowed to plot the evolution of carbon and oxygen peaks characteristic of poly(EHA) and PPF (Figure 5). As expected, with the increase of reaction time the surface composition changes toward the reference poly(EHA) indicating that longer immersion induces more efficient grafting. The amount of grafted chains, reflected by the COO amount (in parallel with the decrease of C═O amount), continuously rises during the first hour of immersion in EHA solution (the same trend for O− and O═ amounts). Afterward, no considerable increase of COO amount is observed probably due to chain end termination or transfer reactions. These transfer reactions might induce formation of transverse ungrafted chains that are most likely washed out during $CHCl_3$ rinsing subsequently to polymerization. Since no further change is observed for longer immersions, the reaction time of 1 h seems to be the optimal compromise of immersion time and grafting efficiency.

Detailed Characterization of the Grafted Chains. Thickness evaluation of poly(EHA) grafted chains can be quite challenging with conventional techniques, such as ellipsometry, because grafted chains and the PPF have very

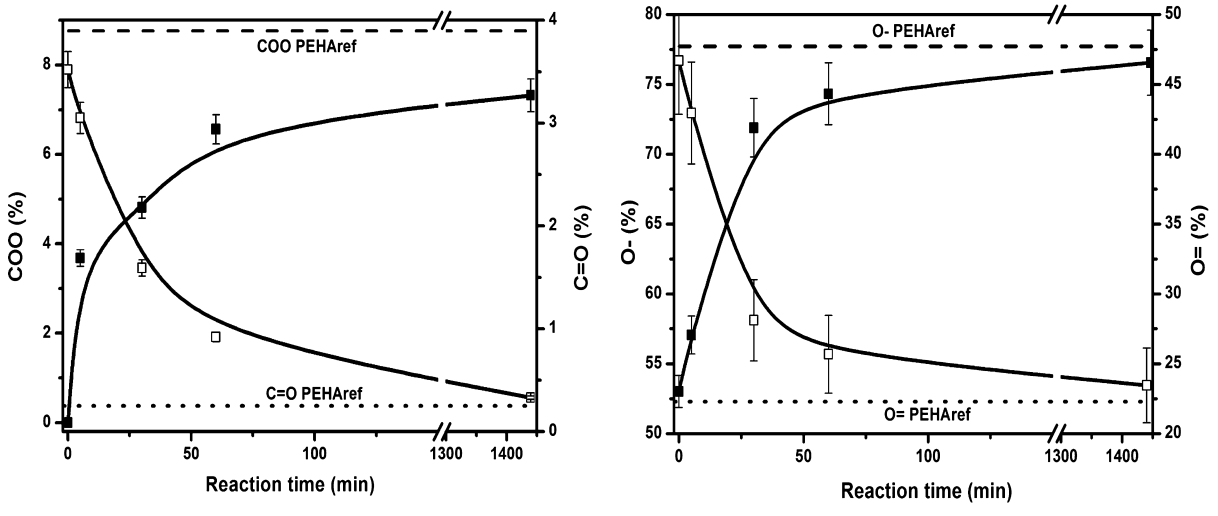

Figure 5. Evolution of (■) COO and O−, and (□) C═O and O═ percentages with immersion time.

close optical properties and refractive indexes are required for any fitting in ellipsometry. An interesting approach to evaluate thickness was considered with the help of XPS. In order to determine the thickness of the grafted layer a method based on angle-resolved XPS (ARXPS) and set up by Cumpson was employed in the current study. This technique is non-destructive and allows to determine elemental and chemical depth profiles of the different species present in the surface of a sample.[31,32]

Taking into account several assumptions including that (1) the sample is considered to be amorphous or finely polycrystalline within the analysis volume, (2) the elastic scattering can be neglected, (3) the refraction of electrons on leaving the specimen surface is negligible, (4) the attenuation length of a photoelectron is independent of the composition of the material through which it passes, (5) the surface of the specimen is smooth and uniform in the *xy*-plane, and (6) the acceptance angle of the electron analyzer (the range of angles over which electrons will be detected) is very small. The formula giving that total photoelectron intensity I corresponding to a particular element can be written as

$$I(\theta) = \phi K \int C(z) \exp\left(\frac{-z}{\lambda \cos \theta}\right)$$

where ϕ is the photon flux, K is a term that takes into account instrumental factors such as transmission function and detector efficiency, $C(z)$ is the function describing the variation of the concentration of the element at depth z, λ is the inelastic free path of the photoelectron, and θ is the takeoff angle of analysis to the normal of the sample. The variation of the takeoff angle will induce a variation of intensity of each element.

In order to interpret ARXPS data, an algorithm set up by Cumpson and further developed by Paynter who created a spreadsheet to fit the model to ARXPS data was used.[31,32] In this model, elemental composition on the surface as well as in the sublayer (substrate or other layer in a multilayer system, for example), fraction of the sublayer coverage, and the photoelectron inelastic free path are all fixed. Then the depth is adjusted to find the best fit of the calculated and experimental data.

Similarly, using the intensities of C1s peak fit components, the thickness of one layer presenting different carbon environment as compared to the underlying layer can be determined.[33] For this particular case, the same inelastic mean free path is inserted for all components of the model.

In the present study, three carbon components, carboxyl group (characteristic of the grafted layer), carbonyl group (characteristic of the of plasma polymer film), and aliphatic carbon component (characteristic of both layers), were considered for the model. Figure 6 displays the ARXPS results obtained from the PPF deposited at 200 W and immersed into EHA for 1 h. It can be seen that the relative intensity of the carboxyl bond increases for higher photoemission angles, indicating that the surface is richer in carboxyl group than the bulk. In the same way, the intensities of aliphatic C−C and carbonyl components decrease for higher photoemission angles, implying that the surface contains less of these groups as compared to the bulk. The model used to fit (solid line) the experimental data (points) assumes that the "sublayer" is characterized by two main components: aliphatic and carbonyl groups with the areas of 96.5% and 3.5%, respectively (PPF composition). The model also assumes that the "top surface" is composed of the other two main components: aliphatic and carboxyl groups with the areas of 91.8% and 8.2%, respectively (poly(EHA) composition). It is also presumed that the fraction of the PPF surface covered by the grafted layer is equal to one implying its homogeneous and full coverage by the polymerized molecules. The best fit of experimental data is shown in Figure 6 and was obtained for the grafted layer thickness of 35 Å.

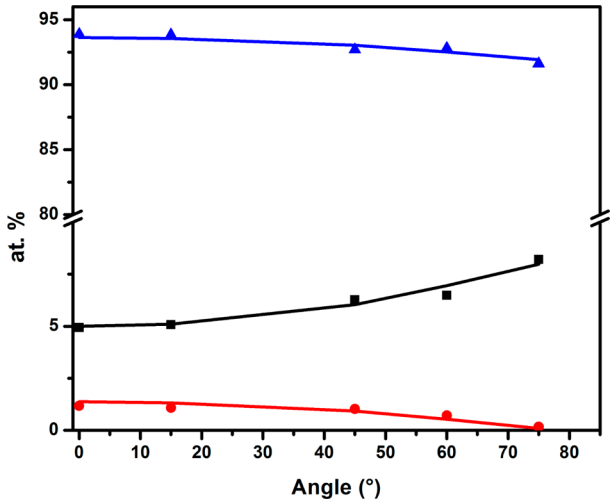

Figure 6. ARXPS fit between the experimental data (points) and the calculation (lines) of the carboxyl (black), carbonyl (red), and aliphatic (blue) groups of the PPF sample deposited at a P_{RF} of 200 W and immersed 1 h in EHA.

The film morphology was characterized by peak force tapping AFM (PFT-AFM). Surfaces of the PPF before and after polymer grafting were imaged with the help of AFM PFT and are presented in Figure 7. Both films do not exhibit any particular features; the morphology is relatively smooth, indicating the surface homogeneity even after poly(EHA) grafting. Moreover, PFT-AFM allows addressing physical properties such as adhesion of the top surface of the film. Adhesion profiles of the as-deposited PPF as well as the PPF with grafted layer are also presented in Figure 7. For the PPF adhesion to the tip ranges between 1.5 and 3.5 nN and significantly increases, up to 11 nN, after grafting suggesting that grafted chains adhere more to the tip than the PPF does. This result can be attributed to the very soft rubberlike state of EHA-based polymers exhibiting low glass transition temperature (T_g) (T_g of bulk poly(EHA) is about −69 °C) as compared to the PPF that is relatively rigid and, thus, does not adhere to the tip. The root-mean-square (RMS) roughness of both samples determined by AFM is about 3 nm. This value is slightly higher than the commonly reported roughness values for the PPF that have a RMS roughness inferior to 1 nm.[34,35] This is probably due to the relatively high thickness of the PPF (500 nm) that could induce some surface reorganization due to mechanical stresses upon exposure to the air.[36,37] For example, Schelz et al. observed that the thick plasma polymer films presented rougher (2.2 ± 0.4 nm) surfaces than the films with a thickness inferior to 400 nm (0.37 ± 0.05 nm).[37]

PPF and PPF with grafted poly(EHA) were also characterized macroscopically by contact angle measurements. The isopropanol-based PPF exhibits a contact angle of ∼85°, indicating a more hydrophilic surface than the bulk poly(EHA) deposited on silicon wafer by spin coating with the contact angle of ∼115°. After grafting, the contact angle of the PPF displays the interfacial behavior of the grafted poly(EHA) with

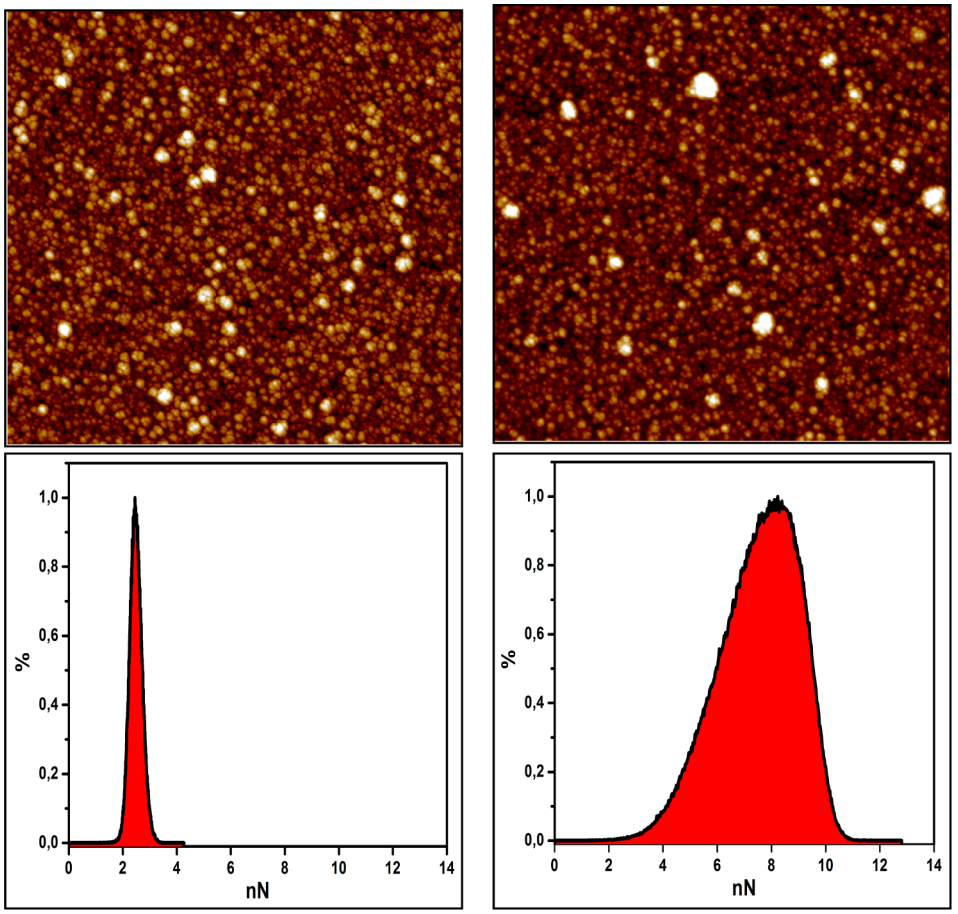

Figure 7. (Top) PFT AFM height images (5.0 × 5.0 μm^2) and (bottom) corresponding adhesion diagrams of the PPF (left) and the PPF on which poly(EHA) chains were grafted (right).

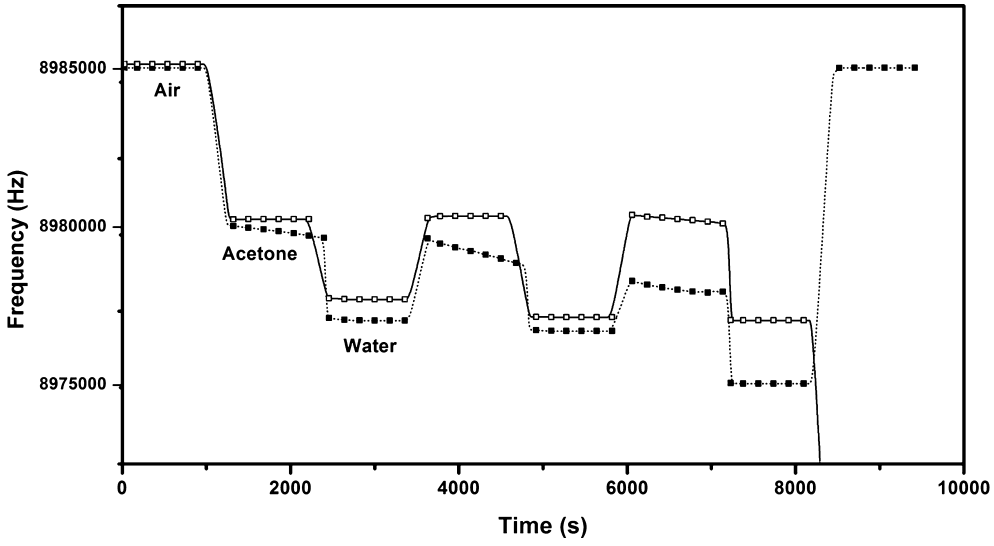

Figure 8. Effect of the solvent on the behavior of the PPF (□) and the PPF with grafted poly(EHA) chains (■).

a value of ~114°. This result indicates that the grafted polymer chains influence the macroscopic behavior of the PPF even though they are quite thin (ca. 3.5 nm as determined by ARXPS). It was also shown that the grafted poly(EHA) layer is homogeneous over the whole surface of the PPF. Moreover, in contrast to conventional methods of plasma functionalization, hydrophobic functions incorporated by grafting of poly(EHA) to the PPF should be relatively stable and, thus, suitable for long time applications. In order to understand better the interfacial behavior and to suggest potential application of the grafted polymer layer protecting PPF against the reoccurring oxidation issue, we investigated the stability of these films upon exposure of different challenging environments including a very good solvent and a nonsolvent of poly(EHA). The PPF

deposited with a P_{RF} of 200 W with grafted poly(EHA) chains was analyzed along with the as-deposited PPF. Each sample underwent three cycles of 20 min in acetone and water; analyses in dry conditions before and after the whole experiment cycles were also performed. QCM, used as a tool to study the mass changes in thin films, was employed in order to monitor the effects of the solvent change. Briefly, for a flat and uniform film firmly attached to a piezoelectric resonator, the change in mass is directly proportional to the change in frequency, as shown in the Sauerbrey equation (eq 1). Therefore, the theoretical frequency decrease caused by adsorption of 1 ng of a substance is about 1 Hz. Figure 8 shows the results of the QCM analyses performed for the two samples. The exposure of the PPF to both solvents has no effect on its behavior during three cycles. Indeed, in both solvents, acetone and water, the frequency is constant during each cycle. A small decrease in water noticed between cycles 1 and 2 suggests only a minor influence of the cycle number on the frequency. After the third cycle a considerable decrease of frequency upon drying and exposure to air as compared to the initial level is observed and it seems that the film is highly swollen. The frequency decrease is associated with the adsorbed mass originating presumably from the PPF uptake of the solvents after a long contact. This behavior was not observed after grafting of poly(EHA) because frequency in air is the same before and after three cycles of exposure. However, in acetone, a good solvent of poly(EHA) chains, a continuous decrease of frequency during cycles 1 and 2 is observed. It confirms that the immersion into acetone induces the solvation of poly(EHA) chains consequently leading to an increase of viscosity close to the quartz crystal. A conformational equilibrium is reached after the third cycle of immersion into acetone once the frequency is stabilized. Upon drying the frequency returns back to its initial value and remains constant during the whole cycle contrary to the nongrafted PPF. The films were solvated by a good solvent of poly(EHA), that is, acetone, and most likely the solvent uptake took place. Therefore, the retained acetone was repelled from the films when they were immersed into water and polymer chains collapsed back because water is a non solvent of poly(EHA). This data indicates that grafting of poly(EHA) chains provides a certain protection to the PPF-based coating.

CONCLUSION

In the current study, an innovative approach based on the initiation of grafting polymerization of 2-ethylhexyl acrylate from the free radicals generated during plasma polymer films synthesis was proposed. Optimization of grafting conditions has shown that the PPF deposited at 200 W contains the highest amount of free radicals available for grafting and 1 h of immersion into in EHA is the optimal immersion time for efficient polymerization. Despite the low thickness of the polymerized layer (3.5 nm), as estimated by ARXPS, QCM analyses have revealed that poly(EHA) grafted chains modify the PPF behavior which in the as-deposited state could be damaged upon exposure to challenging environments. This approach contributes to shaping the path toward new smart nanocoatings through the fine-tuning of the PPF and/or grafted layer composition. Accurate compositional control might result in the enhancement of mechanical and corrosion protection properties as well as in the incorporation of functional properties such as self-healing, pH- or thermoresponsiveness, and so on.

AUTHOR INFORMATION

Corresponding Authors

*E-mail: Youssef.Habibi@umons.ac.be.
*E-mail: Philippe.Dubois@umons.ac.be.

Notes

The authors declare no competing financial interest.

ACKNOWLEDGMENTS

The authors are grateful to the "Région Wallonne" and European Community (FEDER, FSE) in the frame of "Pôle d'Excellence Materia Nova" and in the excellence program OPTI²MAT for financial support. CIRMAP thanks the "Belgian Federal Government Office Policy of Science (SSTC)" for general support in the frame of the PAI-6/27. The authors also thank Dr. M. Debliquy from University of Mons for his help with QCM analyses, Dr. D. Cossement from Materia Nova for Tof-SIMS analyses, Dr. Philippe Leclère for help in AFM images, and Dr. F. Benard for general help.

REFERENCES

(1) Jesch, K.; Bloor, J. E.; Kronick, P. L. *J. Polym. Sci., Part A: Polym. Chem.* **1966**, *4*, 1487−1497.
(2) Kronick, P. L.; Jesch, K. F.; Bloor, J. E. *J. Polym. Sci., Part A: Polym. Chem.* **1969**, *7*, 767−772.
(3) Makhlouf, A. S. H., Tiginyanu, I., Eds. *Nanocoatings and Ultra-Thin Films: Technologies and Applications*; Woodhead Publishing: Cambridge, 2011; Vol. *45*, p 428.
(4) Friedrich, J. *Plasma Process. Polym.* **2011**, *8*, 783−802.
(5) Hiratsuka, A.; Karube, I. *Electroanal.* **2000**, *12*, 695−702.
(6) Park, Z. T.; Choi, Y. S.; Kim, J. G.; Boo, J. H. *J. Mater. Sci. Lett.* **2003**, *22*, 945−947.
(7) Yasuda, H. *Plasma Polymerization*; Academic: Orlando, FL, 1985; p 432.
(8) Smith, D. L. *Thin Film Deposition - Principles and Practice*; McGraw-Hill: New York, 1995; p 616.
(9) Ohring, M. *Materials Science of Thin Films - Deposition and Practice*; Academic Press: San Diego, CA, 2002; p 794.
(10) Gengenbach, T. R.; Chatelier, R. C.; Griesser, H. J. *Surf. Interface Anal.* **1996**, *24*, 271−281.
(11) Gengenbach, T. R.; Vasic, Z. R.; Li, S.; Chatelier, R. C.; Griesser, H. J. *Plasmas Polym.* **1997**, *2*, 91−114.
(12) Gengenbach, T. R.; Vasic, Z. R.; Chatelier, R. C.; Griesser, H. J. *J. Polym. Sci., Part A: Polym. Chem.* **1994**, *32*, 1399−1414.
(13) Gengenbach, T. R.; Griesser, H. J. *J. Polym. Sci., Part A: Polym. Chem.* **1999**, *37*, 2191−2206.
(14) Siow, K. S.; Britcher, L.; Kumar, S.; Griesser, H. J. *Plasma Process. Polym.* **2006**, *3*, 392−418.
(15) Badey, J. P.; Espuche, E.; Sage, D.; Chabert, B.; Jugnet, Y.; Batier, C.; Duc, T. M. *Polymer* **1996**, *37*, 1377−1386.
(16) Jie-Rong, C.; Wakida, T. *J. Appl. Polym. Sci.* **1997**, *63*, 1733−1739.
(17) König, U.; Nitschke, M.; Pilz, M.; Simon, F.; Arnhold, C.; Werner, C. *Colloids Surf., B* **2002**, *25*, 313−324.
(18) Shi, L. *Eur. Polym. J.* **2000**, *36*, 2611−2615.
(19) Shi, L. *React. Funct. Polym.* **2000**, *45*, 85−93.
(20) Teare, D. O. H.; Schofield, W. C. E.; Garrod, R. P.; Badyal, J. P. S. *Langmuir* **2005**, *21*, 10818−10824.
(21) Long, Z. L.; Zhou, Y. C.; Xiao, L. *Appl. Surf. Sci.* **2003**, *218*, 124−137.
(22) Vassallo, E.; Cremona, A.; Laguardia, L.; Mesto, E. *Surf. Coat. Technol.* **2006**, *200*, 3035−3040.
(23) Khelifa, F.; Druart, M.-E.; Habibi, Y.; Bénard, F.; Leclère, P.; Olivier, M.; Dubois, P. *Prog. Org. Coat.* **2013**, *76*, 900−911.
(24) Khelifa, F.; Druart, M.-E.; Habibi, Y.; Rioboo, R.; Olivier, M.; De Coninck, J.; Dubois, P. *J. Mater. Chem. A* **2013**, *1*, 10334−10344.

(25) Ershov, S.; Khelifa, F.; Dubois, P.; Snyders, R. *ACS Appl. Mater. Interfaces* **2013**, *5*, 4216−4223.
(26) Briggs, D.; Seah, M. P. *Practical Surface Analysis by Auger and X-ray Photoelectron Spectroscopy*; John Wiley & Sons: Chichester, England, 1983; p 533.
(27) Chu, J.-Y.; Hsu, W.-S.; Liu, W.-R.; Lin, H.-M.; Cheng, H.-M.; Lin, L.-J. *Procedia Eng.* **2012**, *36*, 571−577.
(28) Pakzad, A.; Simonsen, J.; Yassar, R. S. *Compos. Sci. Technol.* **2012**, *72*, 314−319.
(29) Steinmann, W. *Z. Phys.* **1961**, *163*, 92−107.
(30) Wilken, R.; Holländer, A.; Behnisch, J. *Macromolecules* **1998**, *31*, 7613−7617.
(31) Cumpson, P. J. *J. Electron Spectrosc.* **1995**, *73*, 25−52.
(32) Paynter, R. W. *Surf. Interface Anal.* **1999**, *27*, 103−113.
(33) Perruchot, C.; Watts, J. F.; Lowe, C.; White, R. G.; Cumpson, P. J. *Surf. Interface Anal.* **2002**, *33*, 869−878.
(34) Muguruma, H.; Kase, Y.; Murata, N.; Matsumura, K. *J. Phys. Chem. B* **2006**, *110*, 26033−26039.
(35) Bazaka, K.; Jacob, M. V. *Mater. Lett.* **2009**, *63*, 1594−1597.
(36) Bélard, L.; Poncin-Epaillard, F.; Dole, P.; Avérous, L. *Eur. Polym. J.* **2013**, *49*, 882−892.
(37) Schelz, S.; Schühler, N.; Richmond, T.; Oelhafen, P. *Thin Solid Films* **1995**, *266*, 133−139.